ACS Catalysis

Letter

pubs.acs.org/acscatalysis

Hexadecylphosphate-Functionalized Iron Oxide Nanoparticles: Mild Oxidation of Benzyl C−H Bonds Exclusive to Carbonyls by Molecular Oxygen

Lei Li,[†] Jiangang Lv,[†] Yi Shen,[†] Xuefeng Guo,[†] Luming Peng,[†] Zaiku Xie,[‡] and Weiping Ding*[,†]

[†]Key Lab of Mesoscopic Chemistry, School of Chemistry and Chemical Engineering, Nanjing University, Nanjing 210093, China

[‡]Shanghai Research Institute of Petrochemical Technology, Shanghai 201208, China

Supporting Information

ABSTRACT: We report here a specially designed catalytic system consisting of hexadecylphosphate-functionalized iron oxide nanoparticles in oil/water biphasic emulsion. The iron oxide nanoparticles act as catalytic centers and the surface-bonded hexadecylphosphates as peripheral units which tune the activity of iron oxide and the access of reactants to the catalytic centers. The catalytic system is highly effective to oxidize the benzyl C−H bonds in a series of compounds to carbonyls exclusively by molecular oxygen under mild conditions. The catalytic process, green and low cost, offers a novel concept to design highly effective catalysts with nanoparticles as active centers and surface-bonded organic phosphates as accelerants for oxidation reactions.

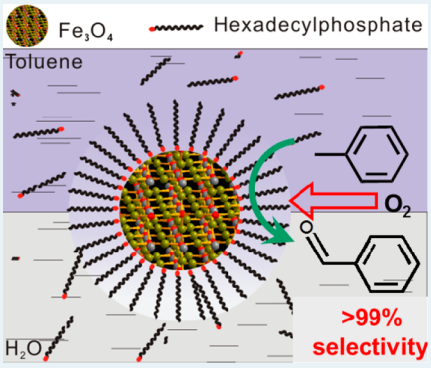

KEYWORDS: *nanoparticles, iron oxide, hexadecylphosphate, selective oxidation, toluene*

1. INTRODUCTION

As an important content of nanoscience, the research on nanocatalysis has been carried out worldwide in the past two decades, and many nanoparticles with well-defined sizes,[1] shapes,[2] and exposed facets,[3,4] including metals,[5−8] bimetallic particles,[9,10] and binary oxides,[11] have shown unique properties as catalysts. The enhancement or adjustment of the catalytic properties of nanoparticles by the electronic and structural interactions among the nanoparticles and supports/ligands is also recognized widely.[12,13] Nanocrystal catalysts are mostly synthesized via colloidal routes in solution with the help of surfactants, ligands, or capping agents which could bind on the particle surface.[14] But in many cases, the surfactants acting as a physical barrier are generally believed to be troublesome for catalytic investigations. From this point, the removal of surfactants from the particle surface before catalytic investigations becomes quite important. Meanwhile, more and more people found that the surfactants or capping agents on particle surface could be utilized as selectivity promotion agents in many catalytic reactions through chiral modification,[15] surface-crowding effect,[16,17] molecular recognition,[18] adsorption regulation,[19] charge-transfer pathways,[20,21] among others. Although qualitative explorations of the promoting roles of capping agents on catalysis have been carried out,[22,23] applying these modifications in the selective oxidation of hydrocarbon is still a challenge.

These explorations have endowed us with an expanded kind of materials active for catalysis. In addition, among the practically important reactions, the introduction of oxygen to organic molecules with super high selectivity has been a big challenge all the time, because the H−C−O units are generally more reactive than the H−C bonds in reactants,[24−26] which causes the overoxidation of products. Similar to the selective oxyfunctionalization of the benzyl H−C bonds by oxygen, the present industrial processes have serious environmental and corrosion problems.[27] Heterogeneous catalytic processes for the reactions have been studied for several decades, of which performance, however, is still far below the demand.[28−30] A significant progress has been reported recently by Hutchings' group that the primary C−H bond in toluene is efficiently oxidized by molecular oxygen to several oxygenates with supported AuPd alloy nanoparticles as catalyst under mild and solvent-free conditions.[9]

Across the spectrum of well-defined nanoparticles (although many of them have been shown to be active to catalyze chemical reactions), however, a single reaction leading to a single product is rare. We think the next step in the catalytic research of nanoparticles toward super performance requires an enhanced understanding of the natural masters of catalysts, such as metalloenzymes. One design developed in our research work has shown promise as a super process for the oxidation of benzyl C−H bonds in a series of compounds exclusive to production by molecular oxygen, in which the nanoparticles of

Received: May 10, 2014
Revised: June 21, 2014
Published: July 16, 2014

   dx.doi.org/10.1021/cs500643r | ACS Catal. 2014, 4, 2746−2752

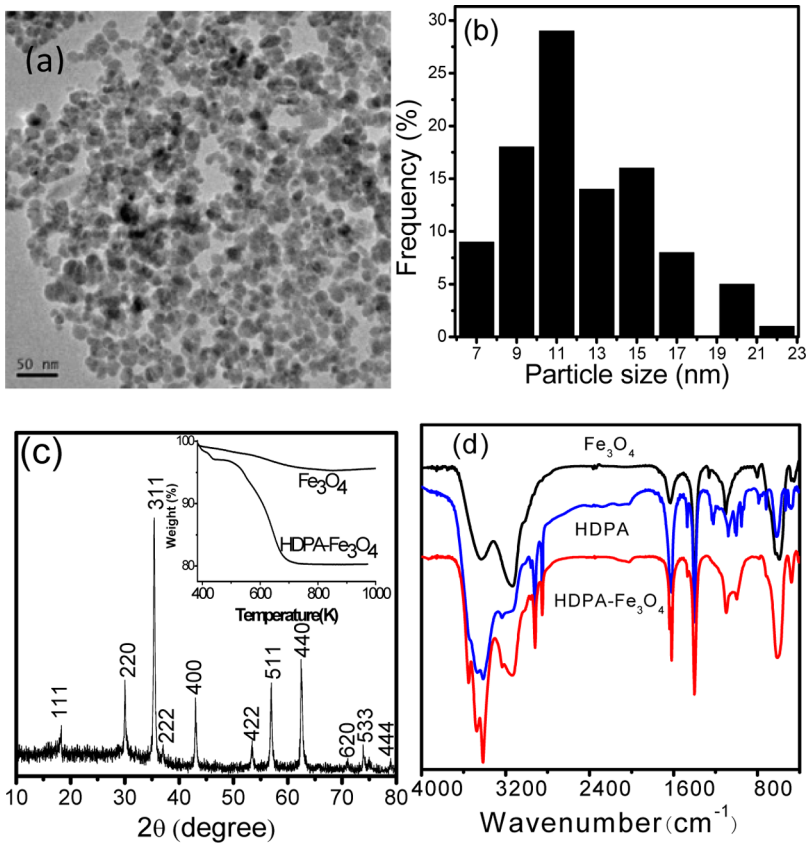

Figure 1. HDPA-Fe_3O_4: (a) TEM image before catalytic test, (b) size distribution of the particles, (c) XRD patterns (inset shows the TG results), (d) FT-IR spectra.

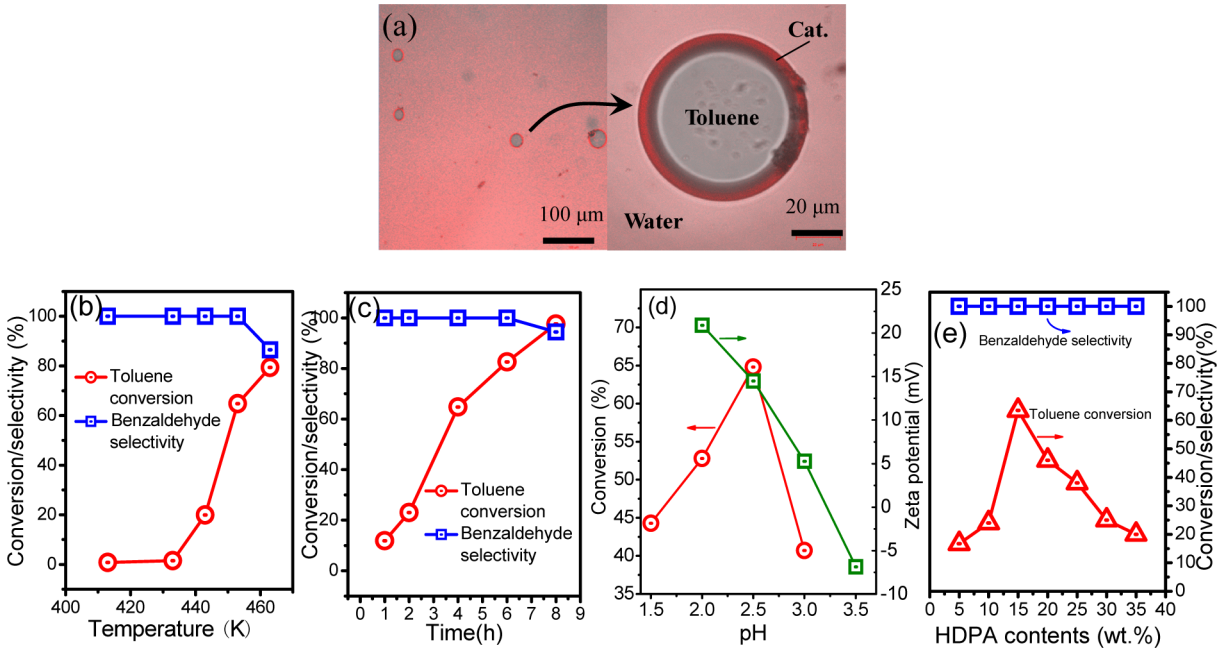

Figure 2. (a) Laser confocal fluorescence photograph of the reaction mixture with small amount of rhodamine B as fluorescence dye adsorbed on the catalyst. Scale bar is 100 μm (left) and 20 μm (right), respectively. The variations of the catalytic property of the catalytic system are shown: (b) with reaction temperature within 4h; (c) with the reaction time at 453 K; (d) pH effects of the system on toluene conversion and zeta potential of the HDPA-Fe_3O_4 nanoparticles; and (e) with the amount of HDPA in the system based on the weight of iron oxide. The reaction time and temperature were fixed for 4 h and 453 K in (d) and (e), respectively. The catalysts used in (e) were prepared in the same method (see Experimental Section) with different amounts of HDPA.

dx.doi.org/10.1021/cs500643r | ACS Catal. 2014, 4, 2746−2752

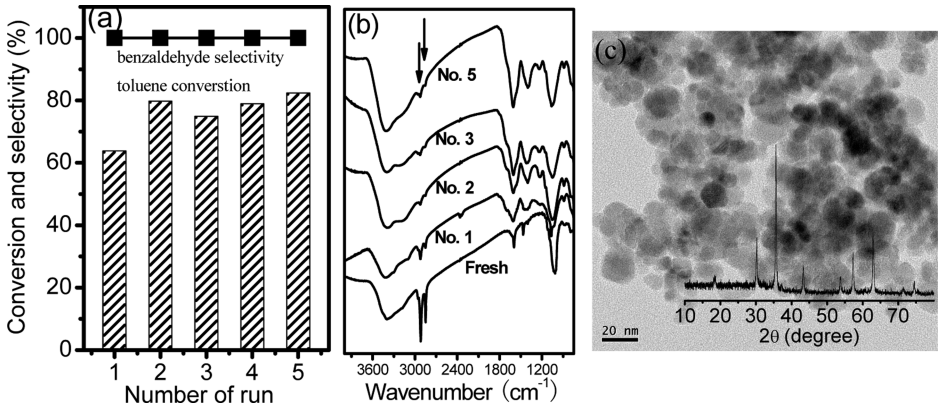

Figure 3. (a) Catalytic properties of the HDPA-Fe_3O_4 during the reuses in long-term operation with an interval of 4 h reactions at 453 K, under 3 MPa O_2. (b) FT-IR spectra of the catalyst after reuses. (c) TEM image of the HDPA-Fe_3O_4 nanoparticles after reaction (inset shows the corresponding XRD patterns).

iron oxide, as catalytic centers, collaborate with peripheral units of hexadecylphosphonic acid (HDPA) and biphasic environments for transfer control to approach the super performance. Such investigation may be the next big thing following nanocatalysis, that is, harnessing multiple weak and strong interactions surrounding the nanoparticles to achieve synergistically super performance.[31]

2. RESULTS AND DISCUSSION

The iron oxide nanoparticles functionalized by HDPA were prepared by modified reverse coprecipitation followed by hydrothermal procedure similar to that listed in refs 32−34. In a typical synthesis, the mixture of aqueous solution of $FeCl_2 \cdot 4H_2O$, $FeCl_3 \cdot 6H_2O$, and HDPA in adequate ratios was added into aqueous ammonia solution at 353 K in a fixed rate of 1.0 $mL \cdot min^{-1}$. The strong adsorption of the HDPA on the surface of iron oxide results in uniform particles with average diameter of ∼12 nm, as exhibited in Figure 1a,b. The XRD patterns (Figure 1c) and IR spectra (Figure 1d) indicate that the synthesized nanoparticles are crystalline Fe_3O_4 coated by HDPA. The sample is named as HDPA-Fe_3O_4 in the context. The naked Fe_3O_4 nanoparticles were prepared using a similar procedure without HDPA in a bit larger particles. The amount of HDPA adsorbed on the iron oxide nanoparticles is determined by TG analysis (inset of Figure 1c) as ∼15 wt %, which can be described as a quasi-bilayer structure with the primary layer strongly bonded to the surface of the Fe_3O_4 nanoparticles.[33] The HDPA adsorption protects the magnetite nanoparticles from surface oxidation in the presence of oxygen and also adjusts the active sites on the surface of iron oxide nanoparticles for the use of catalysis, which eliminates the surface sites too active for selective oxidation (Supporting Information, Figure S1).

The oxidation of toluene by molecular oxygen was performed in a Teflon-lined reactor, and the mixture of toluene and water is in a state of oil-in-water (O/W) emulsion with the HDPA-functionalized iron oxide nanoparticles placed at the interface of the O/W emulsion as stabilizers. The fluorescence photograph of the reaction mixture indeed displayed an O/W emulsion system clearly with the HDPA-Fe_3O_4 catalyst nanoparticles positioned at the interface of the emulsion (Figure 2a). For chemical analysis, a sufficient amount of ethanol was added to destroy the emulsion after reaction and led to homogeneous solution with catalyst particles suspended. A small amount of ethylbenzene was also added as an internal standard to calibrate conversion. The results are listed in Figure 2. The benzaldehyde is the only product analyzed by gas chromatography. The effects of reaction temperature and time on the catalytic performance are shown in Figure 2b,c. The optimal reaction temperature is 453 K, and higher temperatures would initiate the homogeneous oxidation by O_2 diradical and lead to byproducts. Under the conditions, a much longer reaction time produces a small amount of benzyl alcohol and benzoic acid as byproducts, coming from the disproportional reaction of benzaldehyde. It should be mentioned that the byproducts are in fact due to the too high conversion of toluene, which destroys the structure of toluene/water emulsion.

The pH value of the water has an influence on the conversion of toluene, as shown in Figure 2d. The optimal pH value is about 2.5, and lower or higher pH will weaken the catalytic activity. It is well-known that the pH value affects the surface electric property of nanoparticles in suspensions, and the dependence of Zeta potential of the HDPA-Fe_3O_4 on pH value is also shown in Figure 2d. It has been reported[35] that the toluene oxidation reaction proceeds in water by hydride (H^-) transfer from toluene to the catalysts, whereas in toluene solution, it is the hydrogen atom ($H\cdot$) instead of hydride (H^-). When pH value is lower than the isoelectric point of HDPA-Fe_3O_4, the surface of the catalyst will be positively charged and beneficial to the transfer of hydride to the catalyst and promote the toluene reaction. An excessively strong acid of the system will cause the surface of the iron oxide to become unstable.

As shown in Figure 2e, the catalyst activity depends on the packing density of HDPA on the surface of iron oxide. An appropriate amount of HDPA is crucial to higher catalytic activity. The dense HDPA molecules act as mass-transfer barrier-blocking reactants to approach the catalyst surface and result in lower catalytic activity. Too little HDPA, however, is not sufficient to build an emulsion system, so the catalytic performance is also low (Figure 2e). The systematic integration of nano active centers, HDPA peripheral and biphasic reaction media are the key points of the super performance process for the oxidation of benzyl C−H bonds exclusive to aldehyde by oxygen.

Figure 3 shows the performance of the catalytic system during the reuses in a long-term operation. In order to avoid the loss of HDPA and catalyst in separation, 0.7 mL of toluene was added to the suspension at intervals of 4 h reactions. The

dx.doi.org/10.1021/cs500643r | ACS Catal. 2014, 4, 2746−2752

Table 1. HDPA-Fe_3O_4-Catalyzed Reaction of Substituted Alkylaromatics to Corresponding Aldehydes or Ketone

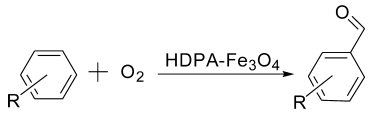

Entry	Substrate	Temp. (℃)	pH	Product	Conv. (%)	Selec. (%)*
1	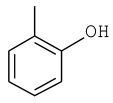	150	2.5	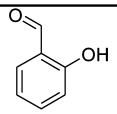	~10	>99
2	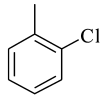	180	2.5	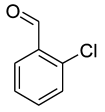	35	>99
3	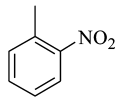	180	2.5	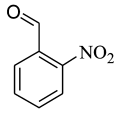	13	>99
4	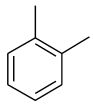	180	2.5	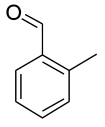	12	>99
5	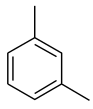	180	2.5	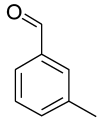	21	>99
6	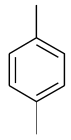	180	2.5	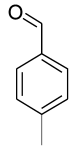	64	>99
7	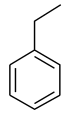	120	5.3	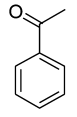	23	>99

*The corresponding product is the only one detected by GC. The reactions were carried out in a 80 mL Teflon-lined autoclave with 1.0 mL of substrate and 0.1 g of catalyst in 40 mL of deionized water under 3 MPa O_2.

results are listed in Figure 3a, which are the sum results of reaction (i.e., the conversion of toluene at the fifth operation is the conversion of the toluene added at the fifth time plus the residual toluene in the former four runs). No separation is carried out during the test. After five runs for a total of 20 h of reaction, the benzaldehyde is still the only product detected by GC, and the HDPA adsorbed on the iron oxide nanoparticles are still stable. For example, the C−H vibrations of HDPA indicated by the arrows are revealed by IR measurement (Figure 3b), which is extremely important for the endurance of the catalytic system[36] and facile to scale up using a reactor operated with continuous separation of the product. The amount of HDPA adsorbed on magnetite nanoparticles during the reaction is determined measured as ~5 wt %, according to the results of TG-DTA measurement performed on the used catalyst. It means that the HDPA adsorption on iron oxide is deficient, leading to the formation of receptors or cavitates for toluene reaction.[37] The morphology of the iron oxide nanoparticles after reactions, depicted as Figure 3c, is similar to that before reaction (Figure 2a). We therefore conclude that the catalytic system is stable for long-term operation and that the exclusive selectivity to aldehyde with high conversion is reliable.

After reaction, the iron oxide is still crystallized in a structure similar to magnetite but in brownish black color and would reasonably change to γ-iron oxide (HDPA-FeO_x) like species in oxygen, which shows identical XRD patterns with the magnetite (inset, Figure 3c), suggesting the protection of HDPA works to some extent even at 453 K in the presence of gaseous O_2. The catalyst is still magnetic and can be separated by a magnet from the suspension (Supporting Information, Figure S2). Although naked Fe_3O_4 nanoparticles were used in the reaction without the promotion of HDPA, no conversion of toluene is detected, and the naked catalyst is found to be α-Fe_2O_3 after the reaction. The property of the iron ions leached into the solution during the reaction is further tested with several designed experiments (Supporting Information, Table

dx.doi.org/10.1021/cs500643r | ACS Catal. 2014, 4, 2746−2752

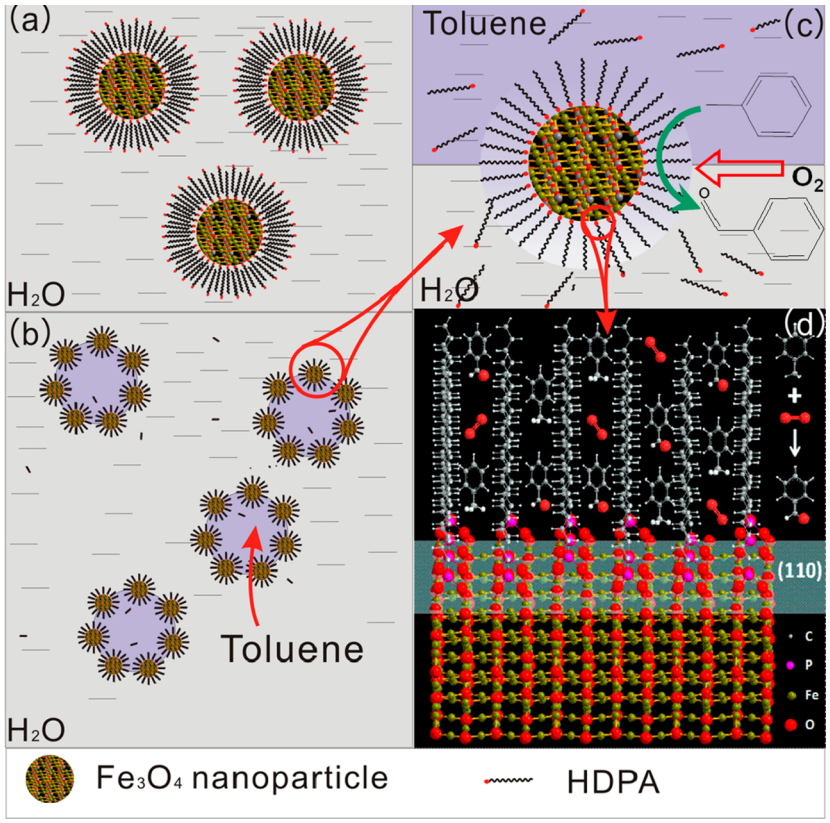

Figure 4. (a) HDPA-Fe_3O_4 nanoparticles synthesized in aqueous solution with quasi double layer of HDPA adsorbed. (b) Oil/water-type dispersion of toluene in water with HDPA-Fe_3O_4 nanoparticles positioned at the interface. (c) Reaction process of toluene to benzaldehyde with oxygen over the HDPA-Fe_3O_4 nanoparticles in the O/W mixed system. (d) Simulated local structure of the iron oxide surface coordinated by HDPA and the access of toluene molecules to the catalytic sites along the lanes of HDPA. The (110) plane of magnetite are shown as an example.

S1). The catalytic activity of leaching iron ions is very low, and the existence of HDPA is also necessary.[38,39]

Besides the oxidation of toluene to benzaldehyde, the current catalytic system works well for the selective oxidation of substituted alkylaromatics to the corresponding aldehydes or ketone with exclusive selectivity under suitable reaction conditions (Table 1). When the strong electron-withdrawing group like $-NO_2$ presented at the benzene cycle, low conversion is obtained. Interestingly, for the three xylene molecules, *o*-, *m*- and *p*-xylene, only one of the two methyl groups can be oxidized into aldehyde group, and the *p*-xylene is the most active substrate with highest conversion during the reaction may be due to its predominance in diffusion originated from its molecular shape.[40]

As a summary, the mechanism of the catalytic system is schematically shown in Figure 4. The structure of HDP-functionalized iron oxide nanoparticles, suspended in water, is depicted in Figure 4a. In the double phases of toluene and water, the nanoparticles of HDPA-magnetite locate themselves at the interface of toluene and water by the hydrophilic/hydrophobic interactions (Figure 4b). The possible oxidation process of toluene to benzaldehyde with oxygen over the HDPA-FeO_x nanopaticles in the O/W mixed system is shown in Figure 4c. The alkyl phosphate molecules not only protect the iron oxide nanoparticles from aggregation and structural change, their long organic chains also help them resident at the interface and promote the access of the alkylaromatics toward the surface of iron oxide by the effect of phase transfer. Moreover, the HDPA appears to shape the alignment of the reactant molecules to contact with the catalyst. The water also plays an important role to transport the oxygen from gas to the reactive liquid phase and the products out of the catalyst. The magnetite nanoparticles with the coordinated hexadecylphosphonic acid stabilized the oil/water biphasic emulsion. The surface-bonded hexadecylphosphonic acid produces a hydrophobic surface and promotes the access of the nonpolar alkylaromatics and the exit of the relatively polar products from the nonpolar surface to the polar environment, which would be the cause of exclusive selectivity.

3. CONCLUSIONS

A super performance catalytic system has been constituted with iron oxide nanoparticles as active centers and the surface-bonded hexadecylphosphates as peripheral units, achieving the conversion of benzyl C−H bonds in a series of compounds exclusive to carbonyls by molecular oxygen under mild conditions. The hexadecylphosphonic acid molecules are extremely important to tune the active surface of the iron oxide for selective oxidation and to promote the access of reactant molecules to the active surface in the O/W reaction emulsion. The unique O/W emulsion with the catalytic nanoparticles locating at the interface of the organic reactants and water leads to highly efficient redox cycle of the catalyst. Compared with the noble metals catalysts used before, the current new system using the base metal oxide as the catalyst is better for industry in scale and, more importantly, offers exclusive selectivity to target compounds. The discovery is instructive for design of catalysts using nanoparticles as catalytic centers leading to super performance.

dx.doi.org/10.1021/cs500643r | *ACS Catal.* 2014, 4, 2746−2752

4. EXPERIMENTAL SECTION

Synthesis of HDPA-Fe_3O_4 Nanoparticles. The HDPA-Fe_3O_4 nanoparticles are prepared using a modified reverse coprecipitation procedure followed by hydrothermal treatment. Typically, 0.40 mmol *n*-hexadecylphosphonic acid (HDPA, Sigma-Aldrich) was dissolved in a mixture of 20 mL of deionized water and 3.0 mLof ethanol at 353 K. Five milliliters of 1.6 M $FeCl_2{\cdot}4H_2O$ and 5.0 mL of 1.6 M $FeCl_3{\cdot}6H_2O$ aqueous solution were added into the HDPA solution slowly. The resulting solution was stirred for 1.5 h. Then, the above solution was added into 80 mL of 1.5 M $NH_3{\cdot}H_2O$ solution in a fixed rate of 1.0 mL·min^{-1} at 353 K and then stirred for another 3 h. The resulting suspension was transferred into a Teflon-lined autoclave and put into an oven at 453 K for hydrothermal treatment of 24 h. The deposit was centrifuged and washed with ethanol and dried in vacuum at 313 K overnight.

Characterization. Powder XRD measurements were performed using a Philips X'Pert MPD Pro X-ray diffractometer with graphite-monochromated high-intensity Cu Kα radiation (0.15418 nm) at 40 kV and 40 mA. TEM images were recorded with a JEM-110 Electron Microscope (JEOL) at an accelerating voltage of 120 kV. HRTEM was performed with a JEOL JEM-2100 instrument at an acceleration voltage of 200 kV. FT-IR spectra were recorded under vacuum condition in a Bruker VERTEX FT-IR spectrometer. TG-DTA analysis was carried on a STA 449C-Thermal Star 300 (Netzsch) in N_2 or air atmosphere to 1073 K.

Catalytic Testing. The toluene oxidation reactions were carried out in an 80 mL Teflon-lined autoclave with 6.6 mmol toluene and 0.1 g of catalyst in 40 mL of deionized water, which performed as dual media for dispersion of and transfer of reactants and products. After purging the reactor three times with oxygen, the temperature of the autoclave was heated up to the reaction temperature, and then 3.0 MPa oxygen was fed to the autoclave, and the oxidation reaction was started. Qualitative determination was carried out using GC-TOF (Micromass, column DB-5) and compared with the authentic samples. Quantitative analysis was performed using Shimadzu GC-2014 gas chromatography equipped with a HP-5 column and FID detector. Ethylbenzene was added after reaction as internal GC standard to calibrate the conversions of reactants.

■ ASSOCIATED CONTENT

Ⓢ Supporting Information

The preparation methods, some characterizations, and related data are shown in Supporting Information. This material is available free of charge via the Internet at http://pubs.acs.org.

■ AUTHOR INFORMATION

Corresponding Author

*E-mail: dingwp@nju.edu.cn. Fax: +86 25 83686251. Tel.: +86 25 83595077.

Notes

The authors declare no competing financial interest.

■ ACKNOWLEDGMENTS

The authors are grateful for the financial support from the Ministry of Science and Technology of China (2009CB623504), the National Science Foundation of China (20673054, 21273107), and Sinopec Shanghai Research Institute of Petrochemical Technology.

■ REFERENCES

(1) Qian, H.; Eckenhoff, W. T.; Zhu, Y.; Pintauer, T.; Jin, R. *J. Am. Chem. Soc.* **2010**, *132*, 8280−8281.
(2) Lee, H.; Habas, S. E.; Kweskin, S.; Butcher, D.; Somorjai, G. A.; Yang, P. *Angew. Chem., Int. Ed.* **2006**, *45*, 7824−7828.
(3) Zhou, K.; Li, Y. *Angew. Chem., Int. Ed.* **2012**, *51*, 602−613.
(4) Xie, X.; Li, Y.; Liu, Z.-Q.; Haruta, M.; Shen, W. *Nature* **2009**, *458*, 746−749.
(5) Oliver-Meseguer, J.; Cabrero-Antonino, J. R.; Domínguez, I.; Leyva-Pérez, A.; Corma, A. *Science* **2012**, *338*, 1452−1455.
(6) Grirrane, A.; Corma, A.; García, H. *Science* **2008**, *322*, 1661−1664.
(7) Chin, Y. H.; Buda, C.; Neurock, M.; Iglesia, E. *J. Am. Chem. Soc.* **2011**, *133*, 15958−15978.
(8) Zhao, D.; Xu, B.-Q. *Angew. Chem., Int. Ed.* **2006**, *45*, 4955−4959.
(9) Kesavan, L.; Tiruvalam, R.; Ab Rahim, M. H.; bin Saiman, M. I.; Enache, D. I.; Jenkins, R. L.; Dimitratos, N.; Lopez-Sanchez, J. A.; Taylor, S. H.; Knight, D. W.; Kiely, C. J.; Hutchings, G. J. *Science* **2011**, *331*, 195−199.
(10) Enache, D. I.; Edwards, J. K.; Landon, P.; Solsona-Espriu, B.; Carley, A. F.; Herzing, A. A.; Watanabe, M.; Kiely, C. J.; Knight, D. W.; Hutchings, G. J. *Science* **2006**, *311*, 362−365.
(11) Yamada, Y.; Tsung, C.-K.; Huang, W.; Huo, Z.; Habas, S. E.; Soejima, T.; Aliaga, C. E.; Somorjai, G. A.; Yang, P. *Nat. Chem.* **2011**, *3*, 372−376.
(12) Schafer, S.; Wyrzgol, S. A.; Caterino, R.; Jentys, A.; Schoell, S. J.; Havecker, M.; Knop-Gericke, A.; Lercher, J. A.; Sharp, I. D.; Stutzmann, M. *J. Am. Chem. Soc.* **2012**, *134*, 12528−12535.
(13) Goel, S.; Wu, Z.; Zones, S. I.; Iglesia, E. *J. Am. Chem. Soc.* **2012**, *134*, 17688−17695.
(14) Niu, Z.; Li, Y. *Chem. Mater.* **2013**, *26*, 72−83.
(15) Gross, E.; Liu, J. H.; Alayoglu, S.; Marcus, M. A.; Fakra, S. C.; Toste, F. D.; Somorjai, G. A. *J. Am. Chem. Soc.* **2013**, *135*, 3881−3886.
(16) Marshall, S. T.; O'Brien, M.; Oetter, B.; Corpuz, A.; Richards, R. M.; Schwartz, D. K.; Medlin, J. W. *Nat. Mater.* **2010**, *9*, 853−858.
(17) Marshall, S. T.; Schwartz, D. K.; Medlin, J. W. *Langmuir* **2011**, *27*, 6731−6737.
(18) Taguchi, T.; Isozaki, K.; Miki, K. *Adv. Mater.* **2012**, *24*, 6462−6467.
(19) Kwon, S. G.; Krylova, G.; Sumer, A.; Schwartz, M. M.; Bunel, E. E.; Marshall, C. L.; Chattopadhyay, S.; Lee, B.; Jellinek, J.; Shevchenko, E. V. *Nano Lett.* **2012**, *12*, 5382−5388.
(20) Jiang, Y.; Yin, P.; Li, Y.; Sun, Z.; Liu, Q.; Yao, T.; Cheng, H.; Hu, F.; Xie, Z.; He, B.; Pan, G.; Wei, S. *J. Phys. Chem. C* **2012**, *116*, 24999−25003.
(21) Tsunoyama, H.; Ichikuni, N.; Sakurai, H.; Tsukuda, T. *J. Am. Chem. Soc.* **2009**, *131*, 7086−7093.
(22) Long, W.; Brunelli, N. A.; Didas, S. A.; Ping, E. W.; Jones, C. W. *ACS Catal.* **2013**, *3*, 1700−1708.
(23) Zhong, R.-Y.; Yan, X.-H.; Gao, Z.-K.; Zhang, R.-J.; Xu, B.-Q. *Catal. Sci. Technol.* **2013**, *3*, 3013−3019.
(24) Gelalcha, F. G. *Chem. Rev.* **2007**, *107*, 3338−3361.
(25) Crabtree, R. H. *Chem. Rev.* **2010**, *110*, 575−575.
(26) Thomas, J. M.; Raja, R.; Gai, P. L.; Grönbeck, H.; Hernández-Garrido, J. C. *ChemCatChem* **2010**, *2*, 402−406.
(27) Satrio, J. A. B.; Doraiswamy, L. K. *Chem. Eng. J.* **2001**, *82*, 43−56.
(28) Raja, R.; Thomas, J.; Dreyer, V. *Catal. Lett.* **2006**, *110*, 179−183.
(29) Brutchey, R. L.; Drake, I. J.; Bell, A. T.; Tilley, T. D. *Chem. Commun.* **2005**, 3736−3738.
(30) Lv, J.; Shen, Y.; Peng, L.; Guo, X.; Ding, W. *Chem. Commun.* **2010**, *46*, 5909−5911.
(31) Service, R. F. *Science* **2012**, *335*, 1167.
(32) Sun, S. H.; Zeng, H. *J. Am. Chem. Soc.* **2002**, *124*, 8204−8205.
(33) Sahoo, Y.; Pizem, H.; Fried, T.; Golodnitsky, D.; Burstein, L.; Sukenik, C. N.; Markovich, G. *Langmuir* **2001**, *17*, 7907−7911.
(34) Yee, C.; Kataby, G.; Ulman, A.; Prozorov, T.; White, H.; King, A.; Rafailovich, M.; Sokolov, J.; Gedanken, A. *Langmuir* **1999**, *15*, 7111−7115.

(35) Gardner, K. A.; Mayer, J. M. *Science* **1995**, *269*, 1849−1851.
(36) Meeuwissen, J.; Reek, J. N. *Nat. Chem.* **2010**, *2*, 615−621.
(37) Xia, Y.; Lim, B. *Nature* **2010**, *467*, 923−924.
(38) Neyens, E.; Baeyens, J. *J. Hazard. Mater.* **2003**, *98*, 33−50.
(39) Voinov, M. A.; Sosa Pagan, J. O.; Morrison, E.; Smirnova, T. I.; Smirnov, A. I. *J. Am. Chem. Soc.* **2011**, *133*, 35−41.
(40) Jones, C. W.; Tsuji, K.; Davis, M. E. *Nature* **1998**, *393*, 52−54.